

# ANALYTICAL PYROLYSIS CHARACTERISTICS OF ENZYMATIC/MILD ACIDOLYSIS LIGNIN FROM SUGARCANE BAGASSE

GAOJIN LV, SHUBIN WU, RUI LOU and QING YANG

*State Key Laboratory of Pulp and Paper Engineering, South China University of Technology,  
Guangzhou, Guangdong, 510640, China*

Received October 16, 2009

The pyrolysis characteristics of enzymatic/mild acidolysis lignin (EMAL) isolated from sugarcane bagasse were investigated by thermogravimetry Fourier transform infrared spectroscopy (TG-FTIR) and pyrolysis gas chromatography mass spectrometry (Py-GC/MS). During thermal analysis, the decomposition of EMAL was found to occur over a wide temperature range, from approximately 150 to 800 °C, while the generated solid residue was of 29% at 900 °C. Two weight loss peaks were recorded at 294 and 385 °C, respectively. The release of gaseous products and of some organic compounds from EMAL pyrolysis, detected on-line using FTIR, occurred mainly between 200 and 500 °C, corresponding quite well with the degradation curves measured by TG. The evolution of CO<sub>2</sub> and organic compounds containing functional groups of C=O and C–O–C marked release peaks mainly at about 300 °C, while the formation of methane, methanol and phenols usually reached the maximum peak at about 400 °C. The phenols can be further divided into G, S and H type derivatives with various substituents, as based on Py-GC/MS results. The basic understanding and insights into lignin pyrolysis and product characteristics will help design the production processes of biofuels.

**Keywords:** sugarcane bagasse, lignin, pyrolysis, TG-FTIR, Py-GC/MS

## INTRODUCTION

With the alarming depletion of fossil energy and increasing awareness of environmental protection, a significant scientific interest is now directed towards the production of biofuel or bioenergy using renewable raw materials. One of the most promising alternatives is the conversion of biomass into char, bio-oils and gaseous products through pyrolysis technologies.<sup>1,2</sup> However, pyrolysis is an extremely complex process, involving a series of reactions, while it can be influenced by many factors.<sup>3</sup> Consequently, it is basically and essentially important to study the pyrolysis characteristics of the three main components in plants (cellulose, hemicellulose and lignin) for a better understanding of biomass thermal chemical conversion. Nowadays, numerous studies<sup>4-6</sup> based on one or all three components have been carried out and most of them were focused on developing kinetic models for predicting the rate of biomass

pyrolysis, while the characterization of the gas and volatiles released during pyrolysis was more rarely performed.

The method of analytical pyrolysis has been considered as a powerful tool for getting pyrolysis characteristics of biomass and of its three main components. As a useful analytical technique to study the pyrolysis behavior of lignin and of other materials, TG-FTIR can not only provide TG parameters, but also analyze the gas releasing properties during the pyrolyzing process. Bassilakis *et al.*<sup>7</sup> developed TG-FTIR quantification routines for infrared analysis of volatile products relevant to seven biomass sample pyrolyses. Lee *et al.*<sup>8</sup> quantified the composition of gases evolving from switchgrass pyrolysis at different heating rates, using FTIR quantitatively. The results show that the major gases were small-molecule ones, such as acetic acid, carbon monoxide, carbon dioxide and ethanol, while

the heating rate did not significantly affect the total amount of gas products. Yang *et al.*<sup>9</sup> investigated the formation characteristics of gaseous compounds from the pyrolysis of three main biomass components (hemicellulose, cellulose and lignin). It was observed that hemicellulose had a higher CO<sub>2</sub> yield, cellulose generated a higher CO yield, and lignin produced higher H<sub>2</sub> and CH<sub>4</sub> yields. Wang<sup>10</sup> and Liu *et al.*<sup>11</sup> also compared the pyrolysis behavior of lignin from different tree species using TG-FTIR analysis, and observed that the pyrolysis of lignins from hardwood released more methanol because of the higher methoxy group content, thus concluding that the difference in the pyrolysis behavior of lignin was due to the different wood species involved in the process.

In this study, the thermal decomposition characteristics of EMAL isolated from sugarcane bagasse (or bagasse for short) together with the gas products releasing behaviors during lignin pyrolysis were studied in detail by TG-FTIR. A better understanding of phenol products was obtained from the further analysis of Py-GC/MS. This fundamental information on the pyrolysis characteristics of EMAL and releasing properties of pyrolysis products is useful for the development of advanced biomass pyrolysis processes for obtaining fuels and valuable organic chemicals.

## EXPERIMENTAL

### Materials

Bagasse obtained from a sugar factory in Guangdong Province, China, was ground in a Willey mill and screened to 40-60 meshes (0.28-0.45 mm). The composition of the bagasse used was as follows: cellulose – 47.8%; hemicellulose – 24.1%; lignin – 18.4% (Klason lignin), ash – 2.2%, on a dry weight basis, obtained according to the method reported by Lawther.<sup>12</sup> The samples were first extracted with a benzene and ethanol (v/v, 2:1) solution for 8 h, to remove the extractives, and then dried in a vacuum oven at 40 °C. The EMAL was isolated by the modified method previously described by Wu<sup>13</sup> and Lou.<sup>14</sup>

### Methods

The elemental analysis of bagasse lignin was performed on an elemental analyzer (Vario-I, Germany).

The experimental TG-FTIR set-up consist of a thermogravimetric analyzer (TGA, NETZSCH STA 499C, Germany) coupled with a FTIR spectrometer (SENSOR 27, BRUKER, Germany). About 15 mg EMAL were heated from 40 to 900

°C at a rate of 20 °C/min in TGA. Purified nitrogen (99.99%) at a flow rate of 40 mL/min was used as carrier gas, to provide an inert atmosphere for pyrolysis and to remove the gaseous and condensable products, thus minimizing any secondary vapor-phase interactions. The gases released in the TGA were purged immediately to a gas cell *via* a Teflon tube, followed by FTIR analysis using a mercury cadmium telluride (MCT) detector, which produces a rapid response at a low noise level (SNR≥32000:1). The transfer line and gas cell were preheated to an internal temperature of 180 °C, to avoid condensation or adsorption of the semi-volatile products. The spectrum scope was located in the 400-4000 cm<sup>-1</sup> range and the resolution factor selected was of 4 cm<sup>-1</sup>.

The Py-GC/MS system includes a JHP-3 model Curie-point pyrolyzer (CDS5200, USA) and an Agilent 6890N gas chromatograph with an Agilent 5973 mass selective detector. A quartz tube was used to load EMAL (about 0.1-0.2 mg) and then placed in the centre of the inductive coil. The pyrolysis chamber was subsequently heated to 600 °C at a rate of 10000 °C/s, then held at 600 °C for 15 s. The products were transferred into the GC *via* a transfer line heated at 270 °C. Other parameters of GC and MS are the following: capillary column – DB-5MS (30 m × 0.25 mm × 0.25 μm); column temperature was first kept at 40 °C for 1 min, then raised to 280 °C, at increments of 10 °C/min, and maintained for 5 min; the injector temperature was of 250 °C with a split ratio of 50:1; the EI ionization energy was of 70 eV, and the scan range was between 33-500 amu, with a scan speed of 1.0 s/decade.

## RESULTS AND DISCUSSION

### Yield and elemental analysis

The yield (based on Klason lignin content) of EMAL isolated from bagasse reached 59.6%, which was much higher than that of MWL separated by aqueous dioxane extraction from finely ball-milled materials, by the classical lignin isolation procedure.<sup>13</sup> Besides, the separation step of enzymatic hydrolysis, followed by mild acidolysis, provided lignin samples of high purity, while minimizing the extent of chemical modification. It is well known that the existence of a lignin carbohydrate complex (LCC) causes difficulties in isolating the pure lignin at a high yield. However, a mild acidolysis treatment after enzymatic hydrolysis can cleave the lignin carbohydrate linkages and recover the lignin with a high yield and purity. The HCl concentration (dioxane/acidified deionized water 85:15 v/v, 0.01mol/L HCl) should be chosen carefully to avoid cleavage of the ether linkages within

the lignin units and also the condensation reactions caused by a high acid content. The elemental analysis results of EMAL are

shown in Table 1, permitting to calculate the O/C and H/C ratio as 0.46 and 1.20 (molar ratio), respectively.

Table 1  
Elemental analysis of bagasse EMAL (%)

Elements	C	H	O*	N
EMAL	57.67	5.78	35.68	0.87

\* calculated by difference

### Thermal analysis

Both TG and DTG curves for pyrolyzing bagasse EMAL, at a heating rate of 20 °C/min, are shown in Figure 1. As shown in the TG curves, the thermal degradation of EMAL proceeded over a wide temperature range, from approximately 150 to 800 °C, which was different from the decomposition of hemicellulose and cellulose, usually occurring over a short temperature range, as reported by Yang *et al.*<sup>15</sup> The fact that lignin contains abundant aromatic rings with various branches, the activity of the chemical bonds and the diverse functional groups in lignin led to EMAL degradation over a wide temperature range. The final charcoal residue yield was of 29% at 900 °C, which can be attributed to the high carbon content in EMAL.

When the temperature was below 150 °C, the weight loss was mainly accounted for by the evaporation of free water. The major pyrolysis occurred between 200 and 500 °C, where two maximum weight loss rates – at 294 and 385 °C, respectively – can be assessed from the DTG curve. This indicates that the bagasse EMAL pyrolysis experiences two rapid reactions over the major mass loss temperature range. Similar trends in the weight loss rates at various heating rates were reported by Lou *et al.*<sup>14</sup> for rice straw lignin, and by Yang *et al.*<sup>16</sup> for wheat straw lignin. A detailed understanding of the evolution characteristics of the pyrolysis products at these two highest degradation rate temperatures will be described later.

### FTIR analysis

Figure 2 shows a typical three-dimensional plot of the FTIR spectra obtained from gas evolving during the pyrolysis of EMAL. As the pyrolysis process maintains a constant heating rate, *i.e.* a different time in the z axis corresponds to a different pyrolysis temperature, the z axis

can also be seen as the temperature axis. Thus, the plane figure consisted of y, while axis z represents the absorbance changes of the wave number selected as a function of temperature, and the plane formed by the x and y axes refers to the IR spectra of pyrolysis products at a specific temperature. From Figure 2, it can be observed that the main gas products of EMAL pyrolysis were: CO<sub>2</sub>, CO, CH<sub>4</sub>, and some organic compounds consisting of phenols, alcohols, ethers (C–O–C), aldehydes and acids (C=O). The release of these products mainly occurred at low temperatures (between 200 and 500 °C), corresponding to the main pyrolysis temperature zone in the TG curve.

The FTIR spectra of the gaseous products generated from the pyrolysis of EMAL at temperatures producing the highest weight loss rate, *i.e.* 294 and 385 °C, respectively, are plotted in Figure 3. Both spectra showed the same absorption bands, except for the differences in absorbance, which indicate that the volatile products released at these two temperatures are different mainly in quantity, but not in type. When pyrolysis proceeded at 294 °C, more gaseous products were released. The absorption bands of water located at 3200-3400 cm<sup>-1</sup> still existed. The characteristic bands of CO<sub>2</sub> between 2270 and 2400 cm<sup>-1</sup> indicated that it was released mostly over this temperature range. The absorbance peaks of CO (2185 cm<sup>-1</sup>) and CH<sub>4</sub> (3024 cm<sup>-1</sup>) appeared in this stage, although in quite small amounts, especially for CO. An intense signal cluster, centered around 1178 cm<sup>-1</sup> (C–O stretching vibrations) and accompanied by signals at 1517 cm<sup>-1</sup> (C=C stretching vibrations) and 1772 cm<sup>-1</sup> (C=O stretching vibrations), strongly indicated the presence of some organic compounds, consisting of phenols, alcohols, aldehydes, esters and acids. Compared to that of 294 °C, the release of CO<sub>2</sub> and of some organic compounds containing functional groups of C=O and C–O–C (1060-1260 cm<sup>-1</sup>)

at 385 °C was weaker, while the formation of phenols and alcohols became stronger. Besides, the absorption bands at 2850-3100  $\text{cm}^{-1}$  had a relatively higher absorbance,

which showed that the hydrocarbons, especially  $\text{CH}_4$ , were mostly generated at high temperature.

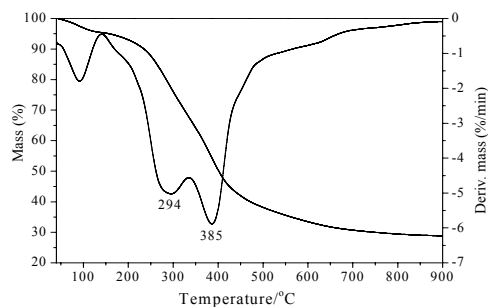


Figure 1: TG and DTG curves of bagasse EMAL

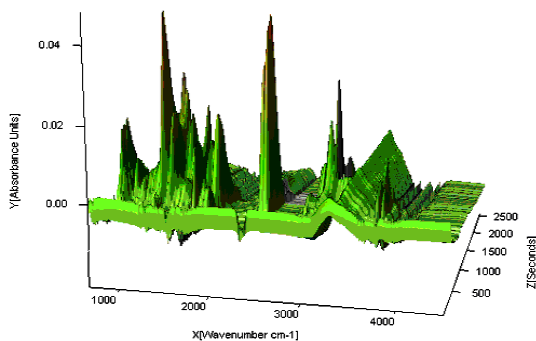


Figure 2: Typical FTIR spectra stack plot from pyrolysis of bagasse EMAL

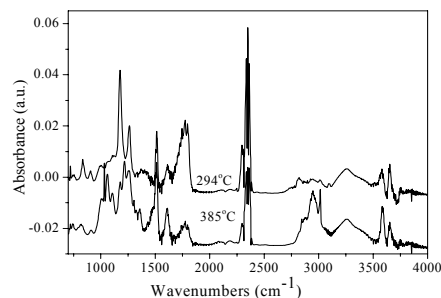


Figure 3: FTIR spectra of pyrolysis products at two maximum volatile release temperatures

### Releasing properties of main gaseous products

The releasing profiles of the gaseous products (such as  $\text{H}_2\text{O}$ ,  $\text{CO}_2$ ,  $\text{CO}$ ,  $\text{CH}_4$ , methanol, phenols and the organic functional bonds of  $\text{C}=\text{O}$  and  $\text{C}-\text{O}-\text{C}$ ) from EMAL pyrolysis are plotted in Figure 4. As the FTIR procedures were the same and absorbance at a specific wave number was linearly dependent on gas concentration, the variation in FTIR absorbance heights can reflect the different product yields of a specific gas species.<sup>7</sup> The specific wave numbers of the FTIR peaks of these products were listed as follows:<sup>10,11</sup>  $\text{H}_2\text{O}$  – 3250  $\text{cm}^{-1}$ ,  $\text{CO}_2$  – 2353  $\text{cm}^{-1}$ ,  $\text{CO}$  – 2185  $\text{cm}^{-1}$ ,  $\text{CH}_4$  – 3024  $\text{cm}^{-1}$ , methanol – 1066  $\text{cm}^{-1}$ , phenols – 1517  $\text{cm}^{-1}$ , organic functional bond  $\text{C}=\text{O}$  – 1738  $\text{cm}^{-1}$  and organic functional group  $\text{C}-\text{O}-\text{C}$  – 1178  $\text{cm}^{-1}$ .

Figure 4a shows that the water release gradually increased with temperature. When temperature was below 200 °C, the water originated mainly from the free and bound water in the EMAL while, at higher

temperature, it was caused by the cracking and reforming of hydroxyl in the aliphatic side chains of lignin. However, the yield of water was relatively low compared to other products. The formation of  $\text{CO}_2$  and  $\text{CO}$ , shown in Figure 4 b-c, probably arose from the decomposition of carboxyl, carbonyl and ether groups in the phenylpropane side chains. The evolution of  $\text{CO}_2$  started at approximately 150 °C, increased rapidly with temperature and reached a maximum at 300 °C. It is worth noting that the release peak temperature (300 °C) was a little higher than that of the first weight loss peak (294 °C), due to the transitional delay between TGA and FTIR. Similar appearances can be seen in Figure 4 d-h. Apart from  $\text{CO}_2$ ,  $\text{CO}$  evolution was observed over a wider temperature range (300-700 °C), with a maximum at about 500 °C, which is in reasonable agreement with the data reported by Wang *et al.*<sup>10</sup> for both Manchurian ash lignin and Mongolian Scots pine lignin. The formation of  $\text{CO}$  over a high temperature range (450-700 °C) was suggested to be

caused by the breaking of the diaryl ether groups and by the secondary pyrolysis of

volatiles.<sup>17</sup>

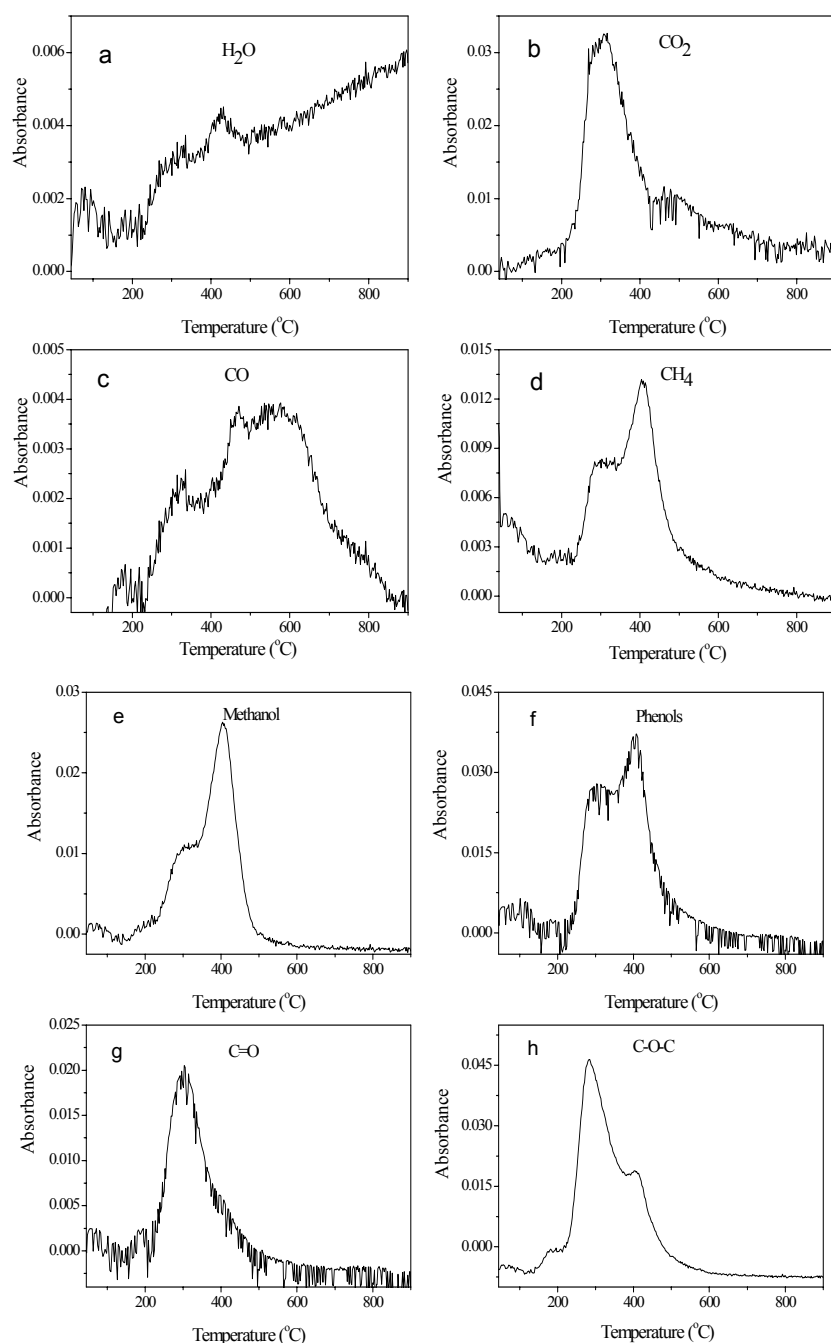


Figure 4: Specific FTIR profiles of gaseous products evolving from bagasse EMAL pyrolysis

The release curve of CH<sub>4</sub>, plotted in Figure 4 d, had two peaks: the former with lower absorbance at 300 °C, the latter at about 400 °C, with much higher absorbance. Then, the CH<sub>4</sub> formation slowly tapered off until about 700 °C. The formation of CH<sub>4</sub> at about 300 °C was caused mainly by the cracking of the methoxyl group (–OCH<sub>3</sub>) on the aromatic rings, while the second peak of evolving CH<sub>4</sub> might be attributed to the

decomposition of the methylene group (–CH<sub>2</sub>–) and to the hydrocarbon skeleton, after deoxygenation. The release profiles of methanol and phenols showed a pattern similar to that of CH<sub>4</sub>, except that their release rates were much higher. With regard to methanol, it was mainly released with cracking of the aromatic methoxyl groups and cinnamyl alcohol-type propanoid side chains.<sup>18</sup> The present results did show two

peaks in the formation of methanol from lignin pyrolysis, which indicates the presence of two methanol sources. As a result of the cleavage of the ether bonds between the lignin building units, followed by cracking and reforming of the alkyl side chains of these units, phenols were released dramatically over a temperature range between 250 and 450 °C. Nevertheless, no specific substance can be identified, due to the limited detection of TG-FTIR. Thus, Py-GC/MS had to be used to get more details on this type of substances.

The formation of organic compounds with bonds of C=O and C–O–C occurred mostly at low temperatures. Compounds with C=O bonds were released in a single peak between 200 and 450 °C, as shown in Figure 4 g, with maxima at about 300 °C. The main component of this type of compounds was formaldehyde, according to Wang *et al.*,<sup>10</sup> who suggested that the formation of formaldehyde was probably attributable to the C<sub>β</sub>–C<sub>γ</sub> cleavage in the alkyl side chains with –CH<sub>2</sub>OH or –COOH groups in –γ position. The release of C–O–C, in Figure 4 h, also shows two peaks, contrary to that of

methanol and phenols, with the first peak, at 300 °C, much higher than the second one, at 400 °C. These results indicate that the C–C bonds connected with carbonyl and ether linkages in the alkyl side chains were weak and could be easily broken to form volatile products including C=O and C–O–C groups at lower temperature. However, at higher temperatures, these carbonyl and ether groups may be further cracked into small molecule gases, such as CO and CO<sub>2</sub>.

### Py-GC/MS analysis

To obtain more information on the individual pyrolysis products generated by the cleavage of the phenylpropane side chains, bagasse EMAL was further subjected to analytical pyrolysis using on-line gas chromatographic/mass spectrometric detection. Figure 5 shows the total ion chromatograms of the EMAL pyrolyzed at 600 °C, and Table 2 summarizes the main pyrolysis products based on NIST 05 mass spectral library and published literature data.<sup>19,20</sup>

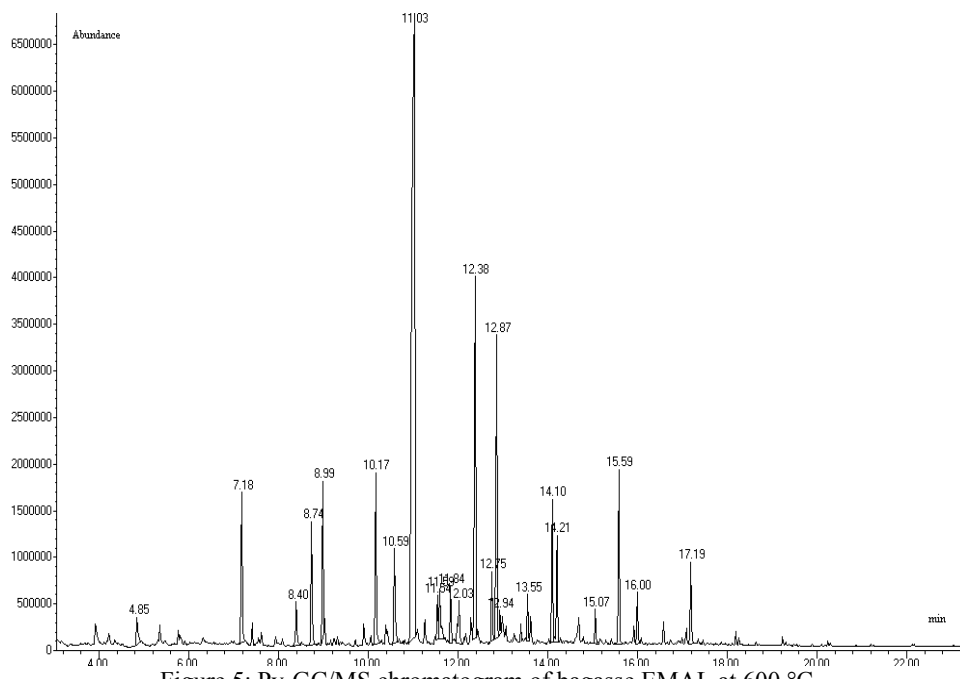


Figure 5: Py-GC/MS chromatogram of bagasse EMAL at 600 °C

It can be noted from Table 2 that a large quantity of monometric phenols was formed, owing to fracture of the ether linkages and C–C bonds contained in the side chains of the lignin polymer. Of all the compounds

observed, furfural can be probably attributed to the decomposition of hemicellulose as impurities. Most of the other products can be classified into molecules with guaiacyl (G units, peaks: 5, 7, 8, 11, 13, 16, 17, 18, 19),

syringyl (S units, peaks: 15, 20, 21, 22, 23) and p-hydroxyphenyl (H units, peaks: 6, 9, 14) aromatic moieties. Besides, there were still some non-specific products observed in the pyrogram, such as phenol, 2-methyl-phenol, 4-methyl-phenol, 3-methoxy-1, 2-benzenediol and 2-allylphenol, which were also formed by the pyrolysis of EMAL, although it is rather difficult to say which aromatic moieties it belonged to. Of these products, 2,3-dihydro-Benzofuran yielded the highest value and was also classifiable as guaiacyl units, according to the hypothesis suggested by Takashi *et al.*<sup>21</sup> – that 2,3-

dihydro-benzofuran is formed through the recombination of the allyl radical intermediate compound during pyrolysis. Jakab and Faix<sup>22</sup> pointed out that the monomer formation was not only determined by the energy required for rupture of the primary bonds (C–C or C–O–C), but it was also decided, even if only to some extent, by H–transfer reactions at high temperature. This conclusion supports the observations that the phenolic compounds contained allyl, vinyl and propenyl (peaks: 12, 13, 14, 19, 22) side chains.

Table 2  
Identification of pyrolysis products

Peak	R.T./min	Compound	Molecular formula	Area pct/%	Match quality/%
1	4.85	Furfural	C <sub>5</sub> H <sub>4</sub> O <sub>2</sub>	0.698	95
2	7.18	Phenol	C <sub>6</sub> H <sub>6</sub> O	2.95	95
3	8.40	2-methyl-phenol	C <sub>7</sub> H <sub>8</sub> O	0.875	97
4	8.74	4-methyl-phenol	C <sub>7</sub> H <sub>8</sub> O	2.43	97
5	8.99	2-methoxy-phenol	C <sub>7</sub> H <sub>8</sub> O <sub>2</sub>	2.505	97
6	10.17	4-ethyl-phenol	C <sub>8</sub> H <sub>10</sub> O	3.162	94
7	10.59	2-methoxy-4-methyl-phenol	C <sub>8</sub> H <sub>10</sub> O <sub>2</sub>	2.052	97
8	11.03	2,3-dihydro-benzofuran	C <sub>8</sub> H <sub>8</sub> O	29.992	87
9	11.54	4-propyl-phenol	C <sub>9</sub> H <sub>12</sub> O	0.728	91
10	11.60	3-methoxy-1,2-benzenediol	C <sub>7</sub> H <sub>8</sub> O <sub>3</sub>	1.256	97
11	11.84	4-ethyl-2-methoxy-phenol	C <sub>9</sub> H <sub>12</sub> O <sub>2</sub>	0.959	89
12	12.03	2-allylphenol	C <sub>9</sub> H <sub>10</sub> O	1.277	96
13	12.38	2-methoxy-4-vinylphenol	C <sub>9</sub> H <sub>10</sub> O <sub>2</sub>	7.384	91
14	12.76	4-(2-propenyl)-phenol	C <sub>9</sub> H <sub>10</sub> O	1.184	96
15	12.87	2,6-dimethoxy-phenol	C <sub>8</sub> H <sub>10</sub> O <sub>3</sub>	6.239	96
16	12.94	Eugenol	C <sub>10</sub> H <sub>12</sub> O <sub>2</sub>	0.313	98
17	13.55	Vanillin	C <sub>8</sub> H <sub>8</sub> O <sub>3</sub>	0.756	96
18	14.10	4-hydroxy-3-methoxy-benzoic acid	C <sub>8</sub> H <sub>8</sub> O <sub>4</sub>	2.339	87
19	14.21	2-methoxy-4-(1-propenyl)-phenol	C <sub>10</sub> H <sub>12</sub> O <sub>2</sub>	1.866	98
20	15.07	4-hydroxy-3,5-dimethoxybenzaldehyde	C <sub>9</sub> H <sub>10</sub> O <sub>4</sub>	0.529	92
21	15.59	4-methyl-2,6-dimethoxybenzaldehyde	C <sub>10</sub> H <sub>12</sub> O <sub>3</sub>	2.942	89
22	16.00	2,6-dimethoxy-4-(2-propenyl)-phenol	C <sub>11</sub> H <sub>14</sub> O <sub>3</sub>	0.878	98
23	17.19	4-hydroxy-3,5-dimethoxyacetophenone	C <sub>10</sub> H <sub>12</sub> O <sub>4</sub>	1.446	94

## CONCLUSIONS

Thermal degradation of EMAL proceeded over a wide temperature range, from approximately 150 to 800 °C, while the final charcoal residue yielded 29% at 900 °C. Two weight loss peaks were recorded on the DTG curve over the major weight loss range, between 200 and 500 °C.

As detected by on-line FTIR, the releasing properties of gaseous products from EMAL pyrolysis matched quite well the degradation curves measured with TG. At low temperatures, under 300 °C, the compounds containing C=O and C–O–C

groups were released quickly due to the C–C bonds breaking in the alkyl side chains, while methane, methanol and phenols were mainly generated at about 400 °C. As discussed above, the cleavage of the methoxyl group gave rise partly to methane and partly to methanol. However, it is still uncertain which one is predominant at present and more experimental work is needed to clarify this.

Many functional groups have been found in the phenols generated, such as methoxyl, alkyl and allyl. Most of these phenols can be classified into G, S and H derivatives,

according to the number of  $-OCH_3$  on the aromatic ring, but the G units still predominate over the EMAL pyrolysis products.

**ACKNOWLEDGEMENTS:** The authors appreciate the financial support provided through the Major State Basic Research Development Program of China (973 Program) (No. 2007CB210201), the National High Technology Research and Development Program of China (863 Program) (No. 2007AA05Z456) and by the National Natural Science Foundation of China (No. 20576043).

#### REFERENCES

- <sup>1</sup> A. V. Bridgwater, D. Meier and D. Radlein, *Org. Geochem.*, **30**, 1479 (1999).
- <sup>2</sup> D. Meier and O. Faix, *Biores. Technol.*, **68**, 71 (1999).
- <sup>3</sup> G. Várhegyi, M. J. Antal, E. Jakab and P. Szabó, *J. Anal. Appl. Pyrol.*, **42**, 73 (1997).
- <sup>4</sup> Q. Yang and S. B. Wu, *Cellulose Chem. Technol.*, **43**, 123 (2009).
- <sup>5</sup> A. Demirba, *Energy Convers. Manage.*, **42**, 1357 (2001).
- <sup>6</sup> J. J. M. Orfão, F. J. A. Antunes and J. L. Figueiredo, *Fuel*, **78**, 349 (1999).
- <sup>7</sup> R. Bassilakis, R. M. Carangelo and M. A. Wójtowicz, *Fuel*, **80**, 1765 (2001).
- <sup>8</sup> S. B. Lee and O. Fasina, *J. Anal. Appl. Pyrol.*, **86**, 39 (2009).
- <sup>9</sup> H. P. Yang, R. Yan, H. P. Chen *et al.*, *Fuel*, **86**, 1781 (2007).
- <sup>10</sup> S. R. Wang, K.G. Wang, Q. Liu *et al.*, *Biotechnol. Adv.*, **27**, 562 (2009).
- <sup>11</sup> Q. Liu, S. R. Wang, Yun Zheng *et al.*, *J. Anal. Appl. Pyrol.*, **82**, 170 (2008).
- <sup>12</sup> J. M. Lawther, R. C. Sun and W. B. Banks, *J. Agric. Food Chem.*, **43**, 667 (1995).
- <sup>13</sup> S. B. Wu and D. S. Argyropoulos, *J. Pulp Pap. Sci.*, **29**, 235 (2003).
- <sup>14</sup> R. Lou and S. B. Wu, *Cellulose Chem. Technol.*, **42**, 371 (2008).
- <sup>15</sup> H. P. Yang, R. Yan and H. P. Chen, *Energ. Fuel.*, **20**, 388 (2006).
- <sup>16</sup> Q. Yang and S. B. Wu, *Cellulose Chem. Technol.*, **43**, 133 (2009).
- <sup>17</sup> O. Faix, E. Jakab, F. Till and T. Szekely, *Wood Sci. Technol.*, **22**, 131 (1988).
- <sup>18</sup> A. Jensen, K. D. Johansen, M. A. Wójtowicz *et al.*, *Energ. Fuel.*, **12**, 929 (1998).
- <sup>19</sup> H. L. Hardell and N. O. Nilvebrant, *Nordic Pulp Pap. Res. J.*, **2**, 121 (1996).
- <sup>20</sup> J. Ralph and R. D. Hatfield, *J. Agric. Food Chem.*, **39**, 1426 (1991).
- <sup>21</sup> H. Takashi, H. Kawamoto and S. Saka, *J. Anal. Appl. Pyrol.*, **84**, 79 (2009).
- <sup>22</sup> E. Jakab, O. Faix and F. Till, *J. Anal. Appl. Pyrol.*, **40**, 171 (1997).